JOURNAL OF MATERIALS SCIENCE 28 (1993) 3439–3443

Synthesis of the B1-type tantalum nitride by shock compression

T. MASHIMO, S. TASHIRO, T. TOYA, M. NISHIDA
Faculty of Engineering, Kumamoto University, Kurokami 2-39-1, Kumamoto 860, Japan
H. YAMAZAKI, S. YAMAYA
Toshiba Tungaloy Co. Ltd, Tsukaguchi 1-7, Saiwai-ku, Kawasaki 210, Japan
K. OH-ISHI, Y. SYONO
Institute for Materials Research, Tohoku University, Katahira 2-1-1, Sendai 980, Japan

B1-type tantalum nitride (polycrystalline bulk state) was synthesized by shock compression. Shock-compression recovery experiments of the porous sample of tantalum nitride with a hexagonal structure (CoSn-type) were performed in the impact-velocity range up to 1.5 km s^{-1}. The instrumental chemical analysis, X-ray and electron diffraction experiments were carried out on the recovered tantalum nitride sample and the combustion-synthesized B1-type sample for comparison. The recovery rate of the B1-type phase increased with increasing porosity, impact velocity and impactor thickness; among these above all the effect of porosity was most remarkable. Almost 100% recovery rate was achieved for the powder of 70% porosity impacted by a 2 mm thick tungsten plate with velocities above 1.4 km s^{-1}. It was confirmed by chemical analysis that the nitrogen content did not change by shock compression. The chemical formulae of the shock-synthesized and combustioned-synthesized B1-type phases were estimated to be $TaN_{0.96-0.99}$ and $TaN_{1.13-1.16,1.27-1.30}$, respectively. The lattice parameter of the shock-synthesized B1-type (Fm3m) phase was $a_0 = 0.43363- + (1)$ nm. The results of X-ray and electron diffraction experiments also supported that the shock-synthesized B1–type tantalum nitride has a good stoichiometry compared with the combustion-synthesized ones.

1. Introduction

At the present time, stoichiometric transition metal nitride with the B1-type structure is theoretically predicted to have a high super-conducting critical temperature [1]. Some nitrides with the same structure are also expected to have high hardness, while the dense-phase boron nitrides whose hardness is next to diamond have been industrially produced by static and shock compressions. The stable phase of tantalum nitride is a hexagonal structure (CoSn–type) under the standard conditions [2]. The B1-type phase tantalum nitride materials have so far been synthesized by means of high pressure [3], high-temperature nitrogen atmosphere [4], self-propagating high-temperature synthesis (combustion synthesis) [5], and plasma-jet synthesis [6]. However, the materials prepared by the first three methods were mixtures with other compounds such as Ta_2N, or consisted of non-stoichometric B1-type phase [3–6]. It was pointed out that the B1-type phase synthesized by the second and third methods contained excess nitrogen atoms [4, 5]. In addition, using the second to fourth methods, bulk materials of the B1-type phase could not be produced.

In this study, shock-recovery experiments of the hexagonal tantalum nitride (powder and sintered lump) were performed to synthesize the B1-type tantalum nitride without denitriding, taking advantage of the very short duration, high pressure and high temperature of the shock wave. The recovered specimens were examined by instrumental chemical analysis, X-ray diffraction and electron diffraction. In addition, B1-type tantalum nitride samples synthesized by combustion synthesis, which had been prepared in the USSR [5] were also investigated for comparison.

2. Experimental procedure

A powder sample of hexagonal-phase tantalum nitride was prepared by nitriding tantalum powder at high temperature at Japan New Metals Co. Ltd and provided by Rare Metallic Co. Ltd. The sample particle has a pole- or plate-like shape about 1 µm long and 0.2 µm wide. These samples were confirmed to consist of the hexagonal phase (CoSn–type), of which the lattice parameters were determined to be $a_0 = 0.51923 + (1)$ nm and $c_0 = 0.29083 + (1)$ nm by powder X-ray diffraction (XRD) method. The nitrogen, oxygen and carbon contents in the samples were found to be 6.63, 0.58 and 0.35 wt %, respectively, by instrumental chemical analyses. Impurities in the original tantalum powder were silicon (0.005 wt %), niobium (0.005 wt %), iron (0.004 wt %), titanium

0022-2461 © *1993 Chapman & Hall*

(0.001 wt %), nickel (0.001 wt %), etc. In addition, the weak XRD lines (for the (1 1 1), (2 0 0) and (2 2 0) planes) of the cubic tantalum carbide (TaC) were detected by increasing the X-ray detector sensitivity; however, the other carbides or oxides could not be detected. The intensities of these lines were consistent with carbon content determined by chemical analysis. It was assumed that oxygen was contained not as bulk tantalum oxides, but as admolecules or surface reaction layers. Owing to the existence of tantalum carbide (TaC) listed in Table I, the chemical formula of the starting material was estimated to be $TaN_{0.97-1.00}$. If oxygen was contained as tantalum oxides in the sample, the fraction of nitrogen should be revised to be slightly larger. The sintered sample was prepared by static compression of 5.5 GPa and 500 °C, by using a belt-type high-pressure apparatus. The porosity of the sintered sample was approximately 13%. Two kinds of B1-type tantalum nitride powders (I and II), which were prepared by a self-propagating high-temperature synthesis under a high-pressure nitrogen atmosphere (combustion synthesis), were provided by the Academy of Science of the USSR [5].

Shock-compression recovery experiments were conducted using a propellant gun [7]. Powdered and sintered samples were enclosed in an iron capsule (SS-21) of about 12 mm inside diameter and 5 mm inside height. Two kinds of samples with different porosities (approximately 56% and 70%) were examined. Shock loading was carried out by impacting the sample capsule with a tungsten flat-flyer plate of 1 or 2 mm thickness, which was accelerated in the range 1.2–1.5 km s^{-1}. The impact velocities were measured by the electromagnetic method [8]. The shock pressure achieved in the sample was estimated by the impedance-matching method from the measured flyer-plate velocity, the Hugoniots of tungsten, steel and the specimen. The Hugoniots of the tantalum nitride powders were roughly estimated from the bulk modulus of tantalum and the porosity value.

TABLE I Instrumental chemical analytical results of nitrogen, oxygen and carbon contents[a]

	Nitrogen (wt %)	Oxygen (wt %)	Carbon (wt %)
Starting material (hexagonal)	6.64[b] 6.61[c]	0.57[b] 0.59[f]	0.36[e] 0.34[d]
Shock-synthesized B1-type	6.59[b] 6.60[c]	0.60[b] 0.68[f]	0.35[e] 0.34[d]
Combustion-synthesized B1-type (I)	8.01[b] 7.89[c]	0.48[b] 0.47[f]	0.05[e] 0.06[d]
Combustion-synthesized B1-type (II)	8.33[b] 8.40[c]	0.89[b] 0.90[c]	0.44[e] 0.42[d]

[a] The measurement errors of nitrogen, oxygen and carbon contents were less than 0.07, 0.02 and 0.01 wt %, respectively.

[b] Measured by the inert gas fusion thermal conductivity method with the EMGA-1200 of Horiba Ltd.

[c] Measured by the inert-gas fusion thermal conductivity method with the TC-436 of LECO Corporation.

[d] Measured by the inert-gas fusion thermal conductivity method with the WR-112 of LECO Corporation.

[e] Measured by the combustion in oxygen non-dispersive infrared absorption method with the EMIA-520 of Horiba Ltd.

[f] Measured by the combustion in oxygen non-dispersive infrared absorption method with the TC-436 of LECO Corporation.

The recovered capsules were carefully peeled out on the lathe. The recovered specimens were investigated using instrumental chemical analysis, powder XRD and electron diffraction. Instrumental chemical analysis of the nitrogen, oxygen and carbon contents was carried out by the inert-gas fusion thermal conductivity method, and the combustion of each in the oxygen non-dispersive infrared absorption method was monitored using two instruments of the EMGA-1200, EMIA-520 of Horiba Ltd, and the TC-436, WR-112 of LECO Corp. The measurements were repeated three or four times for each specimen. The experimental error in the nitrogen, oxygen and carbon contents was estimated to be less than 0.07, 0.02 and 0.01 wt %, respectively, in experiments using Si_3N_4 and TiN standard samples. Powder XRD analyses were carried out using monochromatized CuK_α radiation with a Rigaku Goniometer. The lattice parameter was refined by the least squares method to better than 0.001% accuracy. Correction of the goniometer was performed by measuring diffraction peaks of standard silicon. Electron diffraction experiments were carried out using a JEOL 2000FX electron microscope, operated at 200 kV and equipped with ± 45° double-tilt holder.

3. Result and discussion

Lump-shaped specimens were obtained from the recovered capsule, and were crushed for the various analyses. Some specimens for chemical analysis were acid treated to exclude iron which was a contamination from the capsule. Fig. 1 shows the powder XRD patterns of the starting material and the recovered specimens for 13%, 56%, and 70% porosity, which were shock-loaded using a 2 mm tungsten impactor with almost the same impact velocities (1.32–1.34 km s^{-1}). The pressures of the first shock state in the powder specimens of 56% and 70% porosity were estimated to be 20 and 12 GPa, respectively. New diffraction lines appeared for the powder samples, although the broad diffraction lines of only the hexagonal phase were seen for the sintered one. The new lines were found to be in good agreement with those of the B1-type structure by means of least squares fitting. The intensities of the new lines increased with increasing porosity, in spite of the lower shock pressure as measured above. It was found that the effect of porosity was most remarkable, while the recovery rate of the B1-type phase also increased with increasing impact velocity and impactor thickness. It was suggested that the hexagonal–cubic phase transition strongly depends on temperature, because the larger porosity was thought to induce the higher temperature under shock compression. This was consistent with the fact that the B1-type phase tantalum nitride had been synthesized as a mixture with Ta_2N using a static high pressure above 3 GPa and a temperature over 1800 °C, whereas

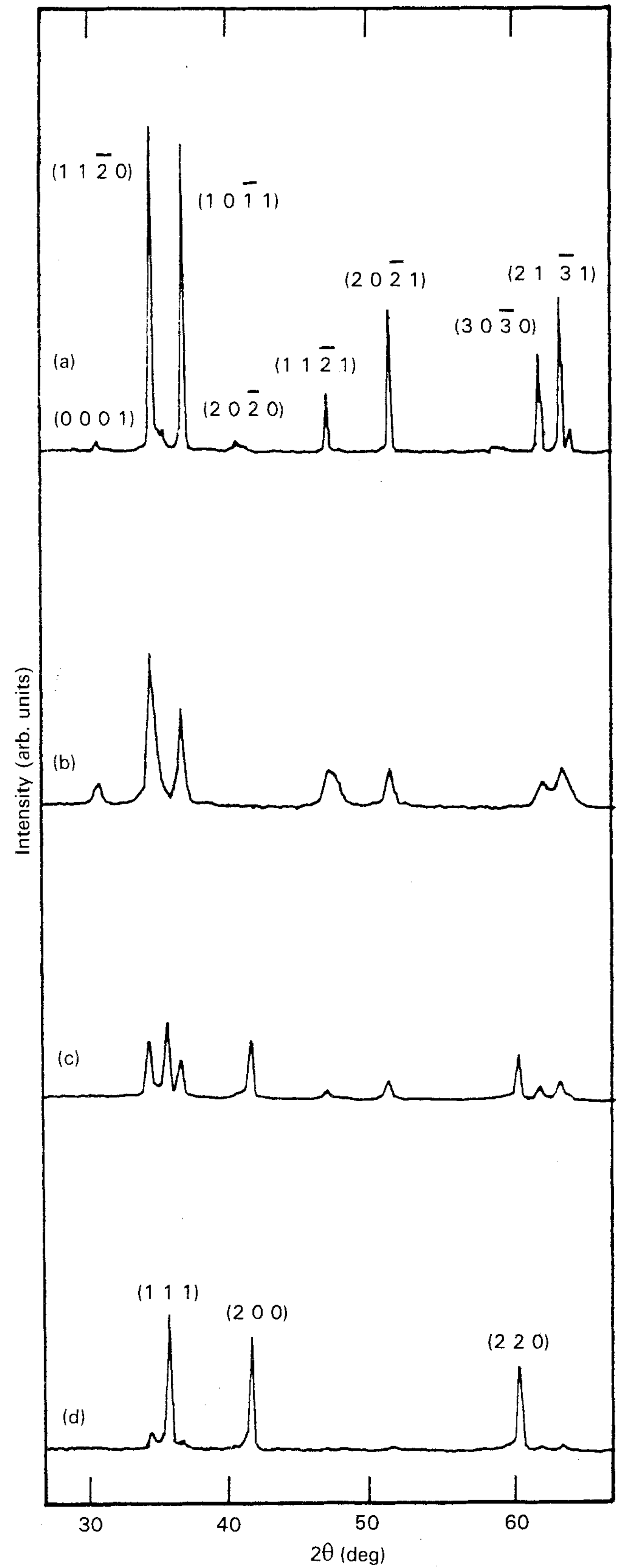

Figure 1 Powder XRD patterns of the starting material and the recovered samples for 13%, 56% and 70% porosity, when the impact velocities of the 2 mm thick tungsten impactor were almost the same (within 1.32–1.34 km s^{-1}). (a) Starting material (hexagonal); (b) Shocked, P_0 = 13%, v_{impact} = 1.326 km s^{-1}; (c) Shocked, P_0 = 56%, v_{impact} = 1.341 km s^{-1}; (d) Shocked, P_0 = 70%, v_{impact} = 1.335 km s^{-1}.

the WC-type hexagonal phase had been synthesized at lower temperatures [3]. Fig. 2 shows the powder XRD pattern of the powder specimen of 70% porosity shock loaded with an impact velocity of 1.474 km s^{-1}.

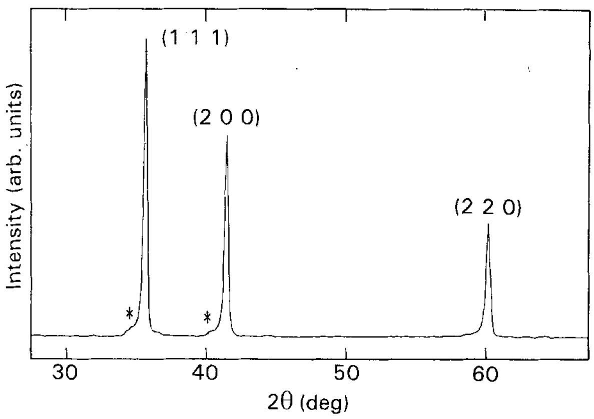

Figure 2 Powder XRD pattern of the recovered specimen for 70% porosity, when the impact velocity of the 2 mm thick tungsten impactor was 1.474 km s^{-1}. The weak X-ray lines, marked *, correspond to those of the cubic-phase tantalum carbide (TaC).

In this shot, no peak of the hexagonal phase was seen, and nearly 100% recovery rate of the B1-type phase was achieved.

The results of chemical analysis of the nitrogen, oxygen and carbon contents of the hexagonal phase sample (starting material), the shock-synthesized B1-type sample (porosity 70%, impact velocity 1.474 km s^{-1}, 2 mm thick tungsten impactor) and the combustion-synthesized B1-type sample are shown in Table I. The nitrogen, oxygen and carbon contents were separately measured using both the Horiba Ltd and LECO Corporation instruments. The data measured by the different instruments were consistent with each other. The nitrogen content of the starting material and the shock-synthesized B1-type sample were almost the same (6.64, 6.61 and 6.59, 6.60 wt %, respectively). The carbon content also did not change (0.36, 0.34 and 0.35, 0.34 wt %, respectively); the amounts were consistent with those estimated by the powder XRD method. However, the oxygen content slightly increased after shock compression (0.57, 0.59 to 0.60, 0.68 wt %, respectively), but the tantalum oxides could not be detected by the powder XRD method. This may be because the specimens adsorbed oxygen as admolecules or surface reaction layers during or after shock compression. Owing to the presence of TaC, the chemical formula of the shock-synthesized B1-type sample was estimated to be $\mathrm{TaN}_{0.96-0.99}$. If oxygen was contained as tantalum oxides in the sample, the fraction of nitrogen should be revised to a slightly larger value. The scatter of the calculated fraction was mainly caused by measurement error of the instrumental chemical analyses of nitrogen. As a result, it was concluded that the nitrogen content did not change on shock compression, and the shock-synthesized B1-type phase had a good stoichiometry. On the other hand, the nitrogen contents of the combustion-synthesized samples (I and II) were found to be around 8.0 and 8.3 wt %, respectively as shown in Table I, which were much higher than the value for the shock-synthesized sample. The chemical formulae of the combustion-synthesized samples (I and II) were estimated by considering the existence of TaC, to be $\mathrm{TaN}_{1.13-1.16}$ and $\mathrm{TaN}_{1.27-1.30}$, respectively.

TABLE II Powder XRD analytical results of the shock-synthesized and combustion-synthesized B1-type tantalum nitride samples

hkl	*d* (obs) (nm)	*d* (calc) (nm)	Rel. deviation (nm)	Intensity (%)	Wave	2θ (obs) (deg)	2θ (calc) (deg)
			Shock-synthesized[a]				
1 1 1	0.250407	0.250359	0.0019	100	Mean	35.860	35.867
2 0 0	0.216709	0.216818	– 0.0050	68	K_{α_1}	41.640	41.618
2 2 0	0.153333	0.153313	0.0013	43	K_{α_1}	60.310	60.319
3 1 1	0.130745	0.130746	0.0000	45	K_{α_1}	72.190	72.190
2 2 2	0.125180	0.125180	0.0000	13	K_{α_1}	75.950	75.950
4 0 0	0.108421	0.108409	0.0011	4	K_{α_1}	90.540	90.553
3 3 1	0.099473	0.099483	– 0.0010	14	K_{α_1}	101.490	101.476
4 2 0	0.096965	0.096964	0.0002	25	K_{α_1}	105.190	105.192
			Combustion-synthesized[b]				
1 1 1	0.249131	0.248979	0.0061	100	Mean	36.050	35.073
2 0 0	0.215621	0.215622	– 0.0001	75	K_{α_1}	41.860	41.860
2 2 0	0.152464	0.152468	– 0.0003	48	K_{α_1}	60.690	60.688
3 1 1	0.130015	0.130025	– 0.0008	36	K_{α_1}	72.660	72.654
2 2 2	0.124472	0.124489	– 0.0014	22	K_{α_1}	75.460	76.447
4 0 0	0.107817	0.107811	0.0005	2	K_{α_1}	91.190	91.196
3 3 1	0.098918	0.098934	– 0.0016	11	K_{α_1}	102.280	102.257
4 2 0	0.096446	0.096429	0.0018	18	K_{α_1}	106.000	106.027

[a] Sys. cubic S.G. Fm3m (225), $a_0 = 0.433\,635$ nm, $V_0 = 81.541 \times 10^{-3}$ nm^3, $\sigma(a_0) = 0.000016$ nm, $\sigma(V_0) = 0.009 \times 10^{-3}$ nm^3

[b] Sys. cubic S.G. Fm3m (225), $a_0 = 0.431244$ nm, $V_0 = 80.199 \times 10^{-3}$ nm^3, $\sigma(a_0) = 0.000024$, $\sigma(V_0) = 0.014 \times 10^{-3}$ nm^3.

The results of XRD analysis of the shock-synthesized and combustion-synthesized B1-type specimens are summarized in Table II. The calculated *d*-spacings were obtained by using the lattice parameter which was determined from the measured *d*-spacing data by the least square method. The X-ray diffraction lines for the shock-synthesized sample were so sharp, that it was easy to distinguish between the fine K_{α_1} and K_{α_2} lines of the (3 1 1), (2 2 2), (4 0 0) lines, etc., in contrast to the combustion-synthesized samples. The lattice parameter of the shock-synthesized sample was determined to be 0.433 63 + (1) nm, while that of the combustion-synthesized sample (I) was 0.431 24 + (2) nm. The calculated *d*-spacings of the shock-synthesized sample showed better agreement with the measured value than did the combustion-synthesized sample (I), as shown in the table.

Fig. 3a and b show the [0 0 1] zone axis for electron diffraction patterns of the shock-synthesized and combustion-synthesized (I) B1-type phases, respectively. The diffraction spots derived from the B1-type structure were only observed in the former. On the other hand, clear superlattice spots were seen in the latter. According to the tilting experiments, these superlattice spots were derived from the long-range ordered (LRO) structure whose unit cell was tetragonal of $a_{\mathrm{LRO}} = 5^{1/2}a_{\mathrm{B1}}$, $b_{\mathrm{LRO}} = 5^{1/2}a_{\mathrm{B1}}$ and $c_{\mathrm{LRO}} = a_{\mathrm{B1}}/2$, and lattice correspondence between LRO and B1 structure was estimated to be as follows:

$$(1\,0\,0)_{\mathrm{LRO}} \text{ and } (0\,1\,0)_{\mathrm{LRO}} \| \{210\}_{\mathrm{B1}},\ [0\,0\,1]_{\mathrm{LRO}} \| [0\,0\,1]_{\mathrm{B1}}.$$

There were six variants of LRO in the B1 matrix, which are divided into three groups with the same habit plane. Therefore, the pattern in Fig. 3b is interpreted as a superimposed pattern of two of six variants with the same habit plane. Further details of this LRO structure are now under study. Considering the larger nitrogen content of the combustion-synthesized sample and the smaller lattice constant (0.431 24 + (2) nm) than that of the shock-synthesized sample

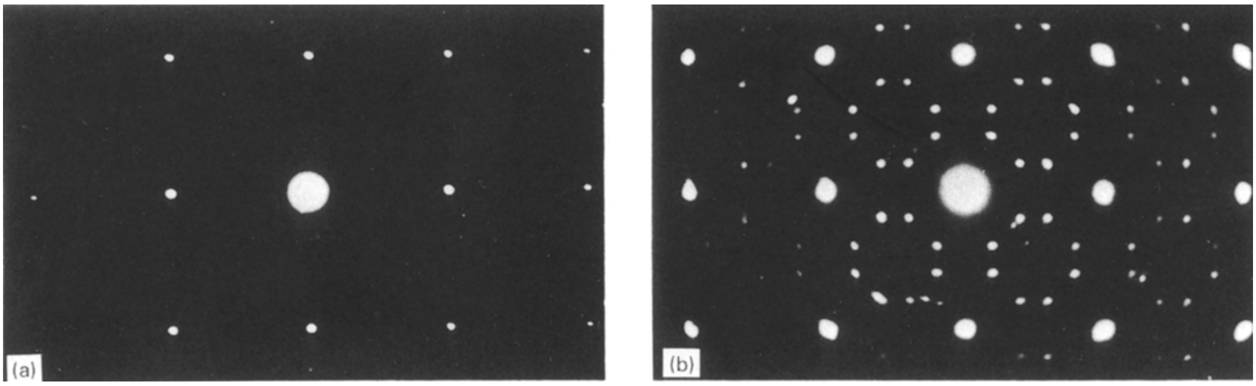

Figure 3 Electron diffraction patterns of (a) the shock-synthesized B1-type tantalum nitride sample and (b) the combustion synthesized sample (I).

(0.433 63 + (1) nm), this LRO structure might relate to that of the ordering of tantalum vacancies.

4. Conclusion

In this study, the B1-type tantalum nitride (polycrystalline bulk state) was synthesized by shock compression of the hexagonal phase (CoSn–type porous material. The recovery rate of the B1-type phase depended strongly on the porosity rate, and almost 100% recovery rate was achieved for the powder specimen of 70% porosity. It was confirmed that the nitrogen content did not change on shock compression. The chemical formulae of the shock-synthesized B1-type phase and combustion-synthesized samples (I, II) were estimated to be $TaN_{0.96-0.99}$ and $TaN_{1.13-1.16, 1.28-1.30}$, respectively.

The X-ray and electron diffraction analyses also supported the finding that the shock-synthesized B1-type phase had a good stoichiometry compared with the combustion-synthesized samples. Because the B1-type tantalum nitride was synthesized without denitriding and with a high recovery rate by shock compression of highly porous starting material, this hexagonal–cubic phase transition might be strongly related to the short duration and high-temperature conditions of shock compression, in addition to the shock stress.

Acknowledgements

The authors thank Horiba Ltd and Japan New Metals Co. Ltd for their helpful support with the instrumental chemical analyses.

References

1. D. A. PAPACONSTANTOPOULOS, W. E. PICKETT, B. M. KLEIN and L. L. BOYER, *Phys. Rev. B* **31** (1985) 752.
2. N. TERAO, *Jpn J. Appl. Phys.* **10** (1971) 248.
3. L. G. BOIKO and S. V. POPOVA, *JETP Lett.* **12** (1970) 70.
4. R. KIEFFER, P. ETTMAYER, M. FREUDHOFMEIER and J. GATTERER, *Monatsch. Chem.* **102** (1971) 483.
5. V. F. PETRUNIN, N. I. SOROKIN, I. P. BOROVINSKAYA and A. N. PITYULIN, *Trans. Poroshkovaya Metall.* **3** (1980) 62.
6. O. MATSUMOTO, E. HAYASHI and Y. KANZAKI, *J. Less Common Met.* **60** (1978) 147.
7. A. NAKAMURA, T. MASHIMO, M. NISHIDA and S. MATSUZAKI, in "Proceedings of the 1989 National Symposium on Shock Waves", edited by K. Takayama (1990) p. 145.
8. T. MASHIMO, in "Proceedings of the 1988 National Symposium on Shock Waves", edited by K. Takayama (1989) p. 105.

Received 15 October 1991
and accepted 25 June 1992